Coordination Chemistry Reviews 282–283 (2015) 127–138

Contents lists available at ScienceDirect

Coordination Chemistry Reviews

journal homepage: www.elsevier.com/locate/ccr

Review

Ru(II) dyads derived from α-oligothiophenes: A new class of potent and versatile photosensitizers for PDT

Ge Shi[a], Susan Monro[a], Robie Hennigar[a], Julie Colpitts[a], Jamie Fong[b], Kamola Kasimova[b], Huimin Yin[a], Ryan DeCoste[a], Colin Spencer[a], Lance Chamberlain[a], Arkady Mandel[b], Lothar Lilge[c,**], Sherri A. McFarland[a,*]

[a] Department of Chemistry, Acadia University, 6 University Avenue, Wolfville, NS B4P 2R6, Canada
[b] Theralase Technologies, Inc., 1945 Queen Street East, Toronto, ON M4L 1H7, Canada
[c] Department of Medical Biophysics, Princess Margaret Cancer Centre/University of Toronto, 101 College Street, Toronto, ON M5G 1C7, Canada

Contents

1. Introduction 128
   1.1. Limitations associated with current PDT approaches 128
   1.2. Metal complexes as PDT agents 128
2. Metal-organic dyads as improved PS constructs for PDT 129
   2.1. Ru(II) dyads as Type I/II PSs 129
   2.2. Ru(II) dyads derived from α-oligothiophenes 129
3. DNA as a therapeutic target 130
   3.1. Overview 130
   3.2. DNA binding 131
   3.3. Photo-triggered DNA damage 131
   3.4. Dual Type I/II photosensitization 133
4. Evaluation in cancer cells 133
   4.1. Nuclear localization 133
   4.2. *In vitro* PDT 135
5. Evaluation in animals: *in vivo* PDT 136
6. Summary and outlook 137
   Acknowledgments 137
   References 137

ARTICLE INFO

Article history:
Received 15 February 2014
Received in revised form 11 April 2014
Accepted 14 April 2014
Available online 24 April 2014

Keywords:
Photodynamic therapy

ABSTRACT

Ru(II) dyads derived from organic units that impart low-lying ^{3}IL excited states combine the most attractive features of organic photosensitizers with those of coordination complexes. The result is a bichromophoric system with excited-state lifetimes that are significantly longer than those associated with traditional ^{3}MLCT states. Incorporation of α-oligothiophenes as the organic chromophore leads to systems that act as dual Type I/II photosensitizers, opening up the possibility of treating hypoxic tumors with photodynamic therapy (PDT) and overcoming problems with *in vivo* dosimetry. These photosensitizers, particularly those that consist of three thiophene units and higher, are remarkable DNA binders

Abbreviations: PDT, photodynamic therapy; PS, photosensitizer; PS*, excited state photosensitizer; ROS, reactive oxygen species; $^1\Delta_g$, singlet oxygen; $^1O_2$, singlet oxygen; O_2, oxygen; ADME, absorption, distribution, metabolism, excretion; bpy, 2,2′-bipyridine; dppn, benzo[*i*]dipyrido[3,2-*a*:2′,3′-*c*]phenazine; ^{3}MLCT, triplet metal to ligand charge transfer; ^{3}IL, triplet intraligand; DNA, deoxyribonucleic acid; Ru(II), ruthenium(II); k_r, radiative rate; k_{nr}, nonradiative rate; eV, electron volt; phen, [1,10]phenanthroline; PI, phototherapeutic index, or photocytotoxicity index; *n*, number of monomeric units; 2*T*, bithiophene; 3*T*, terthiophene; n*T*, *n* linked thiophene units; IP-TT, 2-(2′,2″:5″,2‴-terthiophene)-imidazo[4,5-*f*][1,10] phenanthroline; $nT^{+\bullet}$, oligothiophene radical cation; $O_2^{\bullet-}$, superoxide; UV, ultraviolet; S_o, ground state singlet; S_n, excited state singlet; IR, infrared; IP, imidazo[4,5-*f*][1,10]phenanthroline; GG, guanine-guanine; BRAF V600E, serine/threonine-protein kinase B-Raf valine→glutamate mutation; K_b, binding constant; NP, nucleotide phosphates; pydppn, 3-(pyrid-2′-yl)-4,5,9,16-tetraaza-dibenzo[*a*, *c*]naphthacene; GSH, glutathione; SOD, superoxide dismutase; mTHPC, meta-tetrahydroxylphenylchlorin; Φ_Δ, singlet oxygen quantum yield; NaN_3, sodium azide; DMSO, dimethylsulfoxide; DABCO, 1,4-diazabicyclo[2.2.2]octane; ALA, δ-aminolevulinic acid; CPP, cell-penetrating peptide; HIV Tat, human immunodeficiency virus trans-activator of transcription protein; dppz, dipyridophenazine; AB, Alamar Blue reagent; t_{hv}, PS-to-light time interval; MTD_{50}, half of the maximum tolerated dose; CW, continuous wave.

* Corresponding author. Tel.: +1 9025851320.
** Corresponding author. Tel.: +1 416 581 8642.
E-mail addresses: llilge@uhnres.utoronto.ca (L. Lilge), sherri.mcfarland@acadiau.ca (S.A. McFarland).

http://dx.doi.org/10.1016/j.ccr.2014.04.012

Photosensitizers
Metal complexes
α-Oligothiophenes
DNA damage
Nuclear targeting

and photocleavers when exposed to light, exhibiting no interference with DNA structural integrity in the absence of a light-trigger. Such light-responsive agents localize in the nuclei of cells without the need for a carrier and produce a potent PDT response with minimal dark toxicity. This phototherapeutic effect translates directly to animals and is superior to the clinical agent Photofrin® in this model. These Ru(II) dyads can be activated with light in the PDT window, despite very low molar extinction coefficients in this region, and this phenomenon can be attributed to the efficiency with which these agents operate. The ability to activate these prodrugs with ultraviolet to near-infrared light marks an unprecedented versatility that can be exploited to match treatment depth to tumor invasion depth without compromising potency, giving rise to photosensitizers for multiwavelength PDT.

1. Introduction

1.1. Limitations associated with current PDT approaches

Photodynamic therapy (PDT) is an elegant method for destroying unwanted cells and tissue, whereby light is used to activate an otherwise nontoxic prodrug, termed a photosensitizer (PS) [1]. PDT is best described as a combination therapy that offers spatial and temporal selectivity through local interactions between a PS, light, and oxygen. Briefly, light absorption by the PS produces a reactive excited state (PS^*) that can participate in electron (Type I) or energy (Type II) transfer with ground state molecular oxygen ($^3\Sigma_g^-$) to form superoxide radical anion and cytotoxic singlet oxygen ($^1\Delta_g$), respectively. The production of a cytotoxic burst of reactive oxygen species (ROS), notably singlet oxygen ($^1O_2$), has proven effective in eliminating tumors and tumor vasculature while also inducing an important immune response. The primary advantage of light-based approaches in treating diseases such as cancer is that guided light delivery confines drug activity to malignant sites, thereby reducing collateral damage to surrounding healthy tissue. Consequently, much higher doses of light-responsive cytotoxic agents can be used while simultaneously eliminating the off-site, dose-limiting side effects caused by conventional systemic chemotherapeutics such as cisplatin [2–4].

Despite the enormous potential that PDT holds, its widespread use has not been realized owing, among other reasons, to the inherent limitations associated with the relatively few clinically-approved organic PSs to date. The phototoxicity elicited by porphyrin-based PSs [1,5] exhibits an absolute dependence on O_2, which precludes activity in hypoxic tissue and compromises *in vivo* clinical dosimetry. In addition, these organic agents suffer from poor water-solubility, prolonged retention in tissues, and photobleaching. The search for improved PSs—specifically, coordination complexes—that do not rely on oxygen to exert a PDT effect is a prolific area of focus, evidenced by a surge in literature reports of such agents in recent years [6–13]. The term phototherapy has emerged to distinguish these newer oxygen-independent strategies [12] from traditional oxygen-mediated PDT; however, PS-mediated phototherapy is a more accurate depiction given that the term phototherapy was first coined to refer to treatment of certain human ailments with light (no PS) [1] and continues to be in widespread use to describe light-only treatments for conditions such as psoriasis. Herein, our use of the term PDT includes both oxygen-dependent and oxygen-independent approaches to light therapy mediated by PSs.

Notwithstanding the identification of numerous metal-based systems that are thought to have superior characteristics relative to existing PDT agents, none of these efforts have translated to new metal-based PDT agents for clinical use in cancer therapy. Plaetzer et al. have convincingly summarized several fundamental problems with current approaches to PS design and subsequent translation to clinical applications in a 2009 article, which is still valid five years later [14]. In order to position PDT as a first-line strategy or as an adjuvant therapy in mainstream cancer treatment, PSs must be developed that are potent and reasonably versatile—and, in the times of personalized cancer medicine, must also be designed with a specific indication in mind. Importantly, PS optimization and clinical development must take place in collaboration with experts in medical biophysics and clinical oncology.

1.2. Metal complexes as PDT agents

Various researchers in the field of coordination chemistry have recognized the importance of metals in medicine and have made significant strides toward introducing PSs with unique molecular scaffolds that address some of the concerns regarding the poor chemical characteristics of clinically-approved, purely organic PSs [6–13]. Typically, the comparisons between these new metal-based PSs and the organic porphyrin or porphyrin-related systems are made using isolated DNA gel electrophoresis experiments. Less often *in vitro* cell-based experiments are undertaken, and rarely do the PSs proceed to *in vivo* animal testing. It is important to recognize that true comparisons between new metal-based PSs and existing clinical agents must include evaluation of physicochemical and pharmacokinetic properties, commonly referred to as ADME: absorption, distribution, metabolism, and excretion [15]. Nevertheless, identification of promising PSs must begin with some rational strategy for improving the properties of current PSs by exploitation of the rich chemistry that metals have to offer.

Four main strategies for producing metal complexes as PSs for PDT have been outlined nicely by Glazer in a recent review [12]. They include: (1) metal complexes that generate $^1O_2$ and thus act as conventional Type II agents, (2) compounds that participate in Type I, oxygen-independent photoprocesses, (3) systems that act as photocaging units, releasing biologically active molecules or inhibitors, and (4) compounds that form photoadducts with DNA (also called phototherapy agents). While it is recognized that the biological macromolecular targets of these four classes depend on factors such as subcellular localization and that protein and lipids could be viable targets, most researchers have focused on DNA damage as a rational target (see §3). We wish to add another category to this list: (5) compounds that act as dual Type I/II agents, either by switching in response to oxygen tension or by partitioning excited state reactivity in response to environmental factors or both. Turro et al. [6] have demonstrated that complexes such as $[Ru(bpy)_2dppn]^{2+}$ (bpy = 2,2′-bipyridine, dppn = benzo[*i*]dipyrido[3,2-*a*:2′, 3′-*c*]phenazine) act as dual agents owing to low-lying ^{3}MLCT and ^{3}IL states that both play a role in the excited state trajectory of this and related complexes. The versatility associated with dual Type I/II agents offers the opportunity to improve *in vivo* dosimetry, particularly for large-volume tumors.

Some metal complexes generate $^1O_2$ with unity efficiency [16,17], and these category (1) systems have the advantage of being photocatalytic, drastically reducing the amount of compound

required to elicit a therapeutic effect. However, they do not overcome the major limitation of the organic PSs, namely, the dependence on molecular oxygen to function. Photocaging release and photoadduct formation, categories (3)–(4), have the clear advantage of mimicking cisplatin's oxygen-independent mechanism of action, but therapeutic doses must be higher as these PSs are consumed stoichiometrically for the production of reactive species as mediators of PDT. Additionally, these PSs are inherently unstable with ambient light exposure, complicating their synthetic preparation, subsequent biological testing, and shelf-life.

Compounds that act via oxygen-independent, Type I mechanisms or dual Type I/II switching, categories (2) and (5), respectively, can be photocatalytic or stoichiometric agents or both. They can in principle act via oxidative or reductive mechanisms, although oxidative photobiological damage is more prevalent—or at least more straightforward to identify and hence most documented [18,19]. It is generally accepted that oxidative DNA damage, whether to nucleobases or in the form of frank strand breaks, is subject to efficient DNA repair mechanisms, and thus less effective for PDT when compared to covalent DNA modification. In practice, our best Type I agents and dual Type I/II (oxidative) agents outperform cisplatin and light-responsive metal complexes that form photoadducts with DNA using *in vitro* and *in vivo* models. Nevertheless, we recognize and emphasize that there is no single ideal PDT agent or class of agents. These categories are best viewed as complementary approaches, whereby the end-clinical setting will dictate which approach is best for a given situation. Moreover, there is no reason why combination PDT, utilizing cocktails of mechanistically distinct PSs, could not be applied.

2. Metal-organic dyads as improved PS constructs for PDT

2.1. Ru(II) dyads as Type I/II PSs

Incorporation of organic chromophores into Ru(II) scaffolds to form bichromophoric systems, or *dyads*, is a convenient strategy for exploiting the best properties of both organic and inorganic PSs. The installation of an additional low-lying excited state of organic triplet character can provide a second mode of photoreactivity, leading to dual switching behavior in ideal systems, and also serves to extend the excited state lifetimes of these dyads relative to traditional Ru(II) complexes that do not invoke ^{3}IL states. The idea that tethered organic chromophores could provide a mechanism for extending the excited state lifetimes of metal complexes was first demonstrated in the 1970s by Wrighton et al. [20–23]. Later, this concept of coupling organic triplets to states of similar spin multiplicity in Ru(II) complexes was exploited by Ford and Rogers to lengthen the typical 1-μs ^{3}MLCT lifetimes of these systems by ten-fold via equilibration with low-lying ^{3}IL states [24]. In *dyad* constructs where ^{3}IL states are substantially lower in energy than their ^{3}MLCT counterparts, excited state equilibration with ^{3}MLCT states is suppressed and lifetimes become extremely long, due to unusually low radiative (k_r) and nonradiative (k_{nr}) decay rates between states of distinctly different configuration. Early systems with pure ^{3}IL states exhibited excited state lifetimes in excess of 150 μs [25–27], and we have extended this concept to include ^{3}IL lifetimes of up to 240 μs [28].

A common organic chromophore that we and others have exploited for dyad construction is pyrene, which has a triplet state energy of 2.10 eV [29,30]. This energy is well-matched for coupling to the ^{3}MLCT state of the Ru(II) moiety and establishing excited state equilibration between the pyrene-based ^{3}IL state and the Ru(II) ^{3}MLCT states [25]. Using an ethynyl spacer to link pyrene to the coordinating 1,10-phenanthroline (phen) ligand lowers the organic triplet to 1.8–1.9 eV [13], depending on the linker position

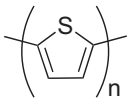

Fig. 1. Basic monomeric unit of α-oligothiophenes, where n = the number of thiophene units.

on the phen ring. A drop in ^{3}IL state energy of this magnitude results in the longest reported lifetimes for Ru(II) dyads to date [28]. Furthermore, these dyads with extremely long lifetimes and correspondingly low values for k_r and k_{nr} serve as potent PSs of *in vitro* PDT. They suffer no loss of function at low oxygen tension, perform well in the presence of PDT attenuators such as melanin, and can be activated with red light. They act as clear Type I/II agents using DNA photodamage as a probe for oxygen-dependence [13]. In fact, the pyrene-based dyads display nanomolar light cytotoxicities with phototherapeutic indices (PI) larger than any previously reported for clinical and nonclinical agents alike. This finding extends to dyads derived from π-expansive organic diimine ligands (dppn) with low-lying ^{3}IL states and long lifetimes. We are intrigued by these findings and particularly interested in testing the scope and boundaries of these and related systems. To this end we turned to organic chromophores with even lower energy triplets—oligothiophenes (Fig. 1).

2.2. Ru(II) dyads derived from α-oligothiophenes

α-Oligothiophenes have garnered significant interest over the last 20 years and continue to be of keen focus, owing to molecular characteristics that become important with higher n. Such oligomers have utility in nonlinear optical applications, for charge storage, and in molecular electronics [31]. In particular, the cationic oxidation states of oligothiophenes represent model systems for the polaronic and bipolaronic charge carriers responsible for electrical conductivity in polythiophenes, an important class of conducting polymers [32]. Even oligothiophenes of smaller n make interesting analogs of polyenes, are good $^1O_2$ generators and biophotosensitizers, and can reductively quench the ^{3}MLCT excited states of Ru(II) complexes [33]. MacDonnell and Wolf [33–35] have exploited reductive quenching in order to achieve long-lived charge separation in Ru(II) dyads with bithienyl-functionalized ligands. Concepts borrowed from the field of photovoltaics and solar energy conversion are especially useful in designing systems for photobiological applications, and we constantly look to the primary literature in these fields for ideas regarding PS improvement for PDT.

The triplet states of bithiophene (2T) as well as longer oligomers with conjugation lengths up to 11 thiophene units (11T) have been identified. The excited state lifetimes of these oligomers range from a few tens of microseconds in fluid solution at ambient temperature to hundreds of microseconds at 77 K [32]. The triplet state energy of 3T has been estimated as 1.72 eV [36], with longer oligomers (4T–11T) having triplet energies that decrease systematically to 1.57 eV following 1/n behavior. These oligothiophene triplets participate in both energy and electron transfer reactions with appropriate acceptors to form $^1O_2$ and nT radical cations ($nT^{+\bullet}$), respectively [32]. The partitioning of this dual reactivity is dictated by chain length and environment and can be utilized to afford dual type I/II PSs for photodynamic applications. The *in vivo* phototoxicity of α-terthienyl (3T) and several of its natural and synthetic derivatives has been attributed to their excellent capacity for generating ROS such as $^1O_2$ and superoxide ($O_2^{\bullet-}$) [36–38]. Plants of the Asteraceae family have evolved to produce this class of secondary metabolites as UV-activatable phototoxins for protection against viruses, bacteria, fungi, nematodes, insects, and the

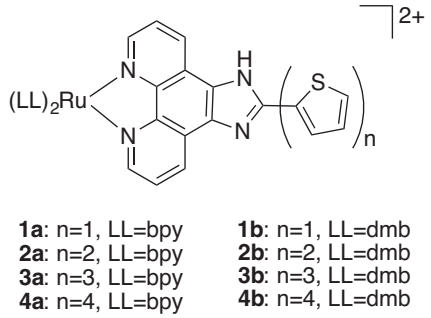

Fig. 2. Molecular structures of Ru(II) dyads derived from thiophene (1*T*) and oligothiophenes (2*T*–4*T*).

eggs and larvae of insects [39]. It is thought that the ROS generated by 3*T* specifically target membrane phospholipids and lipoproteins, leading to lipid peroxidation and ultimately cell lysis [40].

A triplet state energy for 3*T* of about 1.72 eV corresponds to a wavelength of approximately 725 nm, falling in the so-called PDT window, 600–850 nm, the range of wavelengths that penetrate tissue most effectively due to low light scattering and minimal interference by endogenous biomolecules, lipids, and water. Similar to what is observed for triplet state energies, the $S_o \rightarrow S_n$ one-photon absorption of oligothiophenes can be tuned by as much as 1.2 eV on going from 2*T* to 5*T* [41]. Right away one can envision using red and near-IR light to access the ^{3}IL 3*T* state directly or increasing *n* to move the ^{1}MLCT absorption to lower energy. The modularity that characterizes coordination complexes provides a convenient handle for making structural changes to achieve the most desirable photophysical and photochemical properties.

Compounds reviewed herein emerged from a systematic investigation of photobiological activity as a function of *n* [42]. We employed either 2,2′-bipyridine (bpy) or 4,4′-dimethyl-2,2′-bipyridine (dmb) as coligands in series *a* and *b*, respectively (Fig. 2). Thiophene 1*T* and oligothiophenes 2*T*–4*T* served as organic triplet units, and these chromophores were incorporated at C2 of the coordinating imidazo[4,5-*f*][1,10]phenanthroline (IP) ligand [17]. A noteworthy example is oligothiophene 3*T* appended to IP, which yields the functional IP-TT ligand (Fig. 3). This particular construct serves a variety of functions in these dyads, but importantly affords a low-lying ^{3}IL state that can contribute to dual photoreactivity. This organic triplet is lower in energy than our previous pyrene-based systems [28,13] and has the added ability to reductively quench excited Ru(III) configurations. Herein we discuss the photobiological properties of **3a** and **3b**, make comparisons to oligothiophene dyads of larger and smaller *n*, and highlight the potential of these PSs as highly versatile and potent PDT agents. A discussion of their photophysical and photochemical properties and implications these profiles have on their mechanistic action is beyond the scope of this review. All experimental details associated with the figures in this review have been reported [42].

3. DNA as a therapeutic target

3.1. Overview

Maintenance of DNA topology is a highly regulated phenomenon that is tightly controlled during representative processes that are crucial to cell survival: replication, transcription, recombination, and chromosome segregation at mitosis [43]. Even the three-dimensional supercoiling that achieves compaction of the extraordinarily large DNA structure is precise as are the incremental changes in superhelicity governed by the topoisomerase enzymes. Consequently, DNA and the enzymes that control its topology are prime therapeutic targets for anticancer agents [44] owing to the extreme sensitivity of all cellular function to the topological state of DNA. Cisplatin covalently cross-links DNA, most often through intrastrand GG lesions, and the inflicted structural distortion locally unwinds the DNA helix and necessarily affects the degree of supercoiling [45–48]. Topoisomerase inhibitors such as Topotecan® and Etoposide® interfere with the activities of Topoisomerase I and II, respectively, by reducing catalytic turnover of the enzyme in the case of Topotecan® and by stabilizing the topoisomerase–DNA complex in the case of Etoposide® [49–51]. In both examples the requisite DNA topological changes mediated by these enzymes cease, causing a loss of control over the degree of superhelicity and cell death.

Covalent DNA cross-linkers and topoisomerase inhibitors/poisons as anticancer agents suffer from the inability to discriminate effectively between healthy and diseased tissue, thereby leading to dose-limiting systemic toxicity and secondary mutagenic side-effects [52,53]. Therefore, significant effort has been expended toward targeted therapies [54,55], whereby some innate property of a malignant cell or tissue is used as a biomarker to confer selectivity to a drug. Examples include the molecular targeting of a specific genetic aberration as well as the exploitation of chemical or physical properties of diseased tissue (hypoxia, acidity, ROS, transporter-overexpression) [56]. The idea that a cytotoxic agent can be turned on by certain molecular interactions or environmental conditions—but not others—is elegant in theory, but can present salient challenges in practice. Molecular targeting is prohibitively expensive, and both physicochemical and molecular targeting put evolutionary pressure on surviving cancer cells. It has been said that all malignant cancers are governed by Darwinian dynamics and that targeted therapy simply does not work [57]. Targeting of the BRAF V600E mutation in the case of advanced melanoma lends support to such arguments given that median response times are notably short at less than 6 months with lethal drug-resistant disease relapse [58].

The use of light as the external stimulus for confining the cytotoxic potential of a prodrug both spatially and temporally to diseased tissue is an attractive alternative that combines the advantages of conventional therapy (without the side-effects) with targeted approaches (without the cost or evolutionary pressure). The challenge here is to develop inactive prodrugs that only interfere with the topological integrity of DNA when activated by light. Long-lived reactive intermediates are somewhat compatible with this strategy in that the prodrug could have low cellular or nuclear uptake and poor DNA affinity while the activated form can be engineered to yield increased cellular/nuclear uptake and enhanced DNA association [12]. To our knowledge there are no examples adhering to this level of rational design *in vitro* or *in vivo*, although significant strides have been made toward the design of light-activated metal complexes that covalently modify DNA [9–12]. The cationic nature of these reported complexes and their inclusion of groove-binding and intercalating diimine ligands facilitate DNA binding in the absence of a light trigger. Nevertheless, their *in vitro* dark toxicities are strikingly low, which could be due to light sensitization of otherwise slow cellular uptake or fast efflux.

When short-lived, highly reactive intermediates govern DNA damage, nuclear targeting and pre-association with DNA become prerequisites owing to very short diffusion distances of the reactive species. The caveat inherent to this latter approach is that non-light-triggered interactions with DNA that alter its topology become a source of dark toxicity. Sensitization of cellular uptake triggered by light or fast efflux kinetics can play an important role in suppressing the dark toxicity that would otherwise arise from strong DNA binding and ensuing topological changes to its tertiary

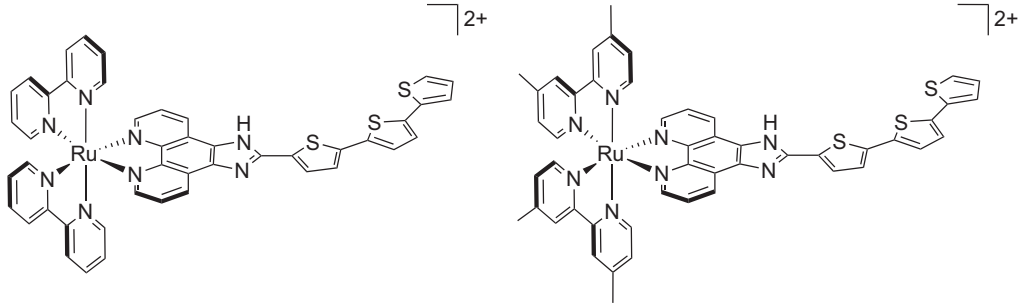

3a: $[Ru(bpy)_2(IP\text{-}TT)]^{2+}$ **3b**: $[Ru(dmb)_2(IP\text{-}TT)]^{2+}$

Fig. 3. Molecular structures of the Ru(II) dyads derived from oligothiophene 3*T*, which are the major emphasis of this review.

structure. Experimentally, we have found that inclusion of relatively non-lipophilic coligands (for slow dark uptake) combined with a non-intercalating functional ligand (to minimize significant dark topological changes to DNA structure) can lead to a strong PDT effect in cells and in animals with much lower dark toxicity compared to the clinically-approved agent Photofrin®, a light-triggered PS that exerts its predominant effect primarily at the cell membrane [1].

3.2. DNA binding

Our group has placed emphasis on octahedral metal complexes derived from two relatively non-lipophilic ancillary ligands (bpy and dmb) that noncovalently associate with DNA very strongly ($K_b \geq 10^7\ M^{-1}$) owing to judicious choice of a third *functional* ligand. In this context *functional* refers to the ligand that imparts DNA binding and is simultaneously responsible for eliciting potent photobiological activity. The low-lying ^{3}IL state supplied by the organic oligothiophene unit is poised to generate singlet oxygen through Type II processes or participate in electron-transfer Type I chemistry via facile formation of the organic-centered radical cation. Its high affinity for nucleic acids ensures that maximal damage occurs at the Ru(II) binding site on the DNA helix upon photoactivation.

For the present series of dyads, association with DNA increases with increasing *n*, with $K_b \sim 10^6\ M^{-1}$ when $n = 1$ and up to $K_b \sim 10^8\ M^{-1}$ when $n \geq 3$ (Fig. 4). The magnitude of ΔT_m from thermal denaturation experiments at [PS]/[NP] = 0.1 and comparison to known DNA intercalators such as ethidium bromide suggests that the oligothiophene-based dyads do not intercalate DNA. Therefore, we infer that groove binding plays an important role in these PS-DNA interactions, and the strength of this association exceeds some of the best known intercalators. High affinity for DNA ensures maximal damage to its structure upon photoactivation of the prodrug, and slow dissociation kinetics positions these PSs for proximal lesions, which are more deleterious and less likely to be repaired by the cellular protective machinery. Importantly, the absence of an intercalating effect for these PSs indicates that topological changes to the DNA structure in the absence of a light trigger may be minimal. Together, non-intercalative binding, slow cellular uptake/fast efflux, and photosensitization of cellular/nuclear uptake could be responsible for their low dark toxicity both *in vitro* and *in vivo*.

3.3. Photo-triggered DNA damage

Light-responsive changes to the topological structure of DNA can be discerned readily by monitoring the electrophoretic mobility of supercoiled plasmid DNA through an agarose gel [59,60]. The relative migration distances of plasmid increase in the order of nicked circular (Form II, single-strand breaks), linear (Form III, two single-strand breaks on opposite strands or one frank double-strand break), and supercoiled (Form I, no strand scission). When DNA intercalation or cross-linking by some exogenous agent leads to unwinding of the helix and concomitant removal of negative supercoils, the migration effect is a gradual retardation of Form I DNA with increasing concentration of agent until the removal of all superhelical structure causes the plasmid to comigrate with Form II DNA [44].

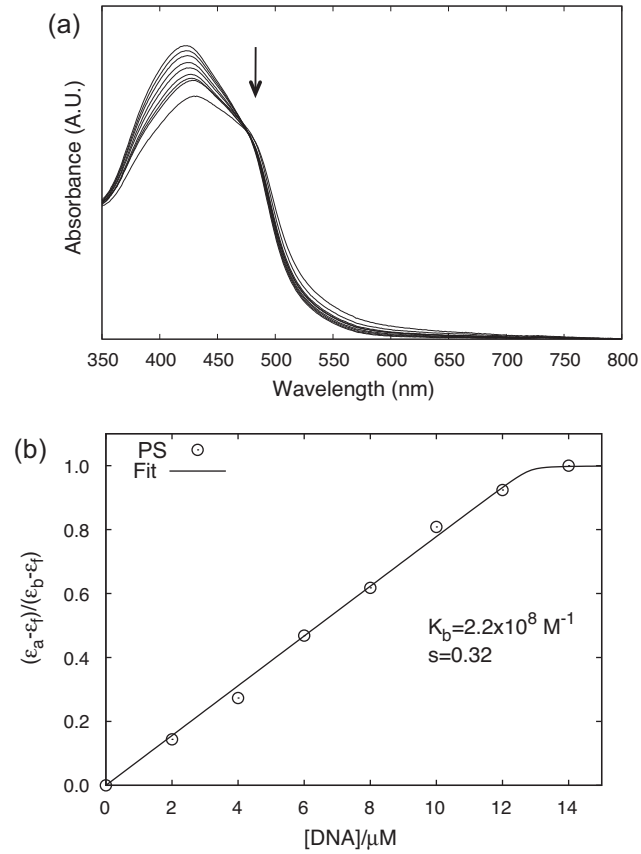

Fig. 4. (a) Optical titration of compound **3a** (50 μM) with CT DNA (2–14 μM bases) in Tris buffer (5 mM Tris·50 mM NaCl) at pH 7.5. (b) Binding isotherm calculated for absorption changes at 419 nm.

Ru(II) dyads derived from α-oligothiophenes do not disrupt the topological integrity of DNA in the absence of a light trigger. However, these agents readily photocleave DNA when exposed to visible light, and the magnitude of this activity increases with increasing *n*. Fig. 5 demonstrates the effect of increasing concentration of **3a** on the topology of plasmid DNA. As little as 500 nM PS (lane 4) has

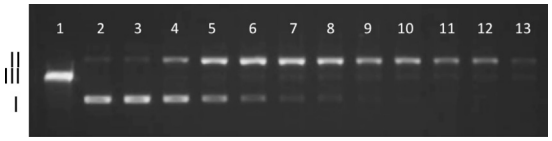

Fig. 5. Agarose gel electrophoresis of pBR322 DNA (20 μM bases in 5 mM Tris, 50 mM NaCl, pH 7.5) with light-activated Ru(II) dyad **3a**. Lane 1, linear pBR322; lanes 2–3, supercoiled pBR322 with and without light, respectively; lanes 4–13, dose–response profile collected for 0.5–5 μM PS. The light dose was 7 J cm^{-2} of visible light (400–700 nm).

a discernible effect on the topological structure of pBR322 DNA, with single-strand breaks beginning to accumulate. Notably, the DNA photocleavage induced by **3a** produces traces of the more deleterious double-strand breaks with increasing PS concentration, confirmed by comigration of the photodamaged DNA with linearized pBR322 (lane 1). As the concentration of **3a** is increased under these conditions, the PS quenches the fluorescence from the ethidium bromide DNA stain used for visualization of the bands, causing bands to fade with increasing concentration of PS. The potency of photo-triggered DNA damage by dyads derived from oligothiophenes with $n \geq 3$ are comparable to some of the most efficient Ru(II)-based photocleavers that yield 100% Form II DNA at PS-to-nucleotide ratios (r_b) as low as 0.2 [6,16]. However, these systems derived from dppn (dppn = benzo[*i*]dipyrido[3,2-*a*:2′,3′-*c*]phenazine) and pydppn (pydppn = 3-(pyrid-2′-yl)-4,5,9,16-tetraaza-dibenzo[*a*, *c*]naphthacene) photoactive ligands do not produce double-strand breaks as observed for the oligothiophene-based series, illustrated for **3a** as the faint Form III DNA bands (Fig. 5).

Interestingly, the formation of double-strand lesions induced by PSs such as complex **3a** is amplified in the presence of endogenous reducing agents such as glutathione (GSH). Fig. 7 compares the photocleavage by **3a** in the absence (a) and in the presence (b) of 10 mM GSH, which reflects the relatively high concentration of this cytoprotective agent in cells [61]. The platinum-based anticancer drugs such as cisplatin are notoriously susceptible to detoxification by GSH due to rapid binding and inhibition of DNA cross-linking. Ru(II) complexes that covalently cross-link DNA with light activation (Fig. 6) have shown the remarkable ability to maintain function in the presence of high concentrations of GSH [9], presumably due to the expectation that Ru(II) is less likely to act as a soft acid toward soft sulfur-containing nucleophiles. The Ru(II) dyads derived from oligothiophenes are not only able to maintain their photobiological activity in the presence of GSH, but importantly, their photodynamic effect is significantly enhanced by GSH.

Careful inspection of Lane 1 (Fig. 7) indicates that double-strand breaks are initiated by the oligothiophene-based Ru(II) complexes in the nanomolar regime with mM concentrations of GSH (b) but not in its absence (a). With GSH and 2 μM (r_b = 0.1) PS, almost all of the plasmid has incurred double-strand breaks (Lane 4) followed by complete degradation at concentrations of PS much less than 5 μM (r_b = 0.25). This ability to form double-strand lesions is not seen at corresponding concentrations of PS in the absence of GSH.

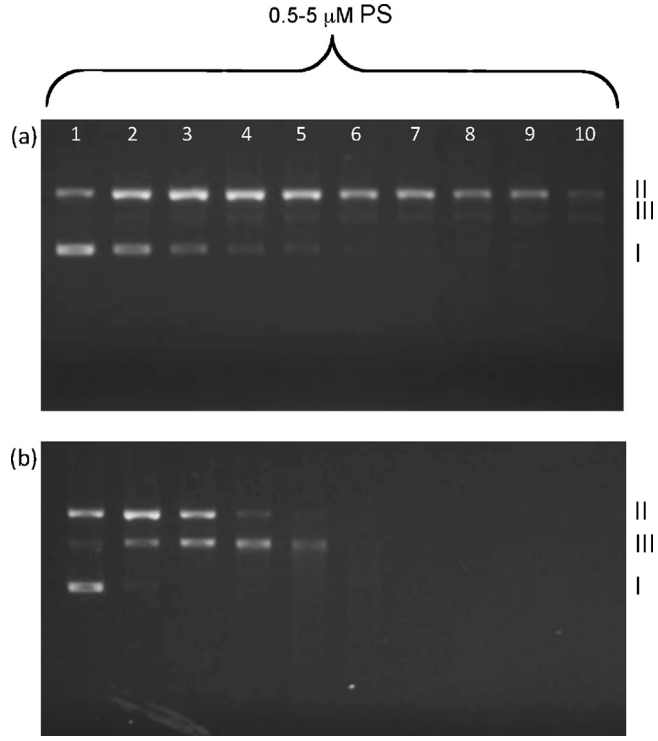

Fig. 7. DNA photocleavage of pBR322 mediated by compound **3a** in the absence (a) and presence of 40 mM GSH (b). The light treatment was 7 J cm^{-2} of visible light (400–700 nm).

At 2.5 μM (r_b = 0.25) and higher, linearized plasmid that has been further degraded (Lanes 5–10) loses its ability to be imaged by the intercalating dye ethidium bromide or residual luminescence from the Ru(II) complex owing to a complete loss of structural integrity. In the absence of a light trigger, DNA damage is minimal in the presence of GSH and Form I predominates (Fig. 5, Lane 2). Facilitation of DNA damage in this series is reduced when n = 2, and there is no effect when n = 1. This direct correlation between increasing n and amplification of phototriggered DNA damage in the presence of GSH extends to other endogenous reductants that commonly act as antioxidants [42].

It has been observed that inhibition of cellular antioxidant pathways increases the sensitivity of cells to PDT [62]. The SOD-1 and GSH pathways have been implicated in reducing the PDT effect by clinical agents such as meta-tetrahydroxyphenyl chlorin (mTHPC). Attenuation of PDT by antioxidants is not unexpected given that the role of such endogenous species is to scavenge ROS and other cytotoxic intermediates that serve as prime mediators of PDT by clinically-approved PSs. Therefore, the facilitation of DNA photodamage by these Ru(II) dyads in the presence of significant concentrations of GSH and various other important antioxidants is surprising and highlights a potentially unique mechanism of action for these potent DNA damaging agents.

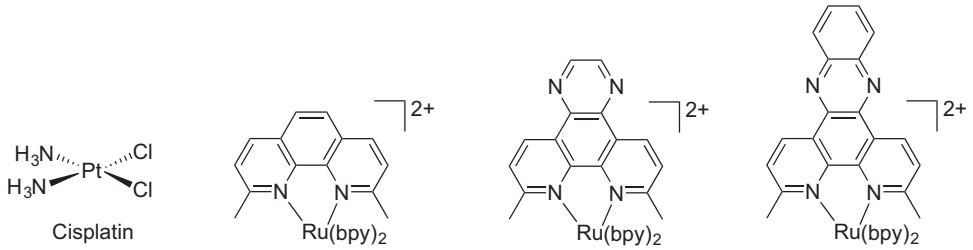

Fig. 6. Structures of cross-linking agents that covalently modify DNA.

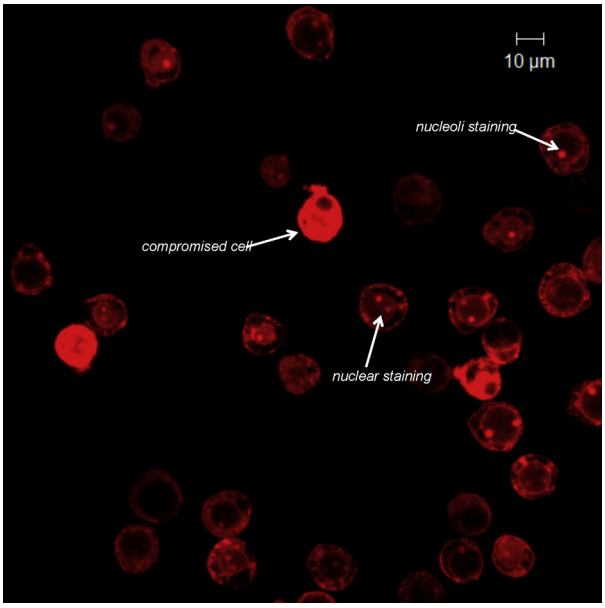

Fig. 8. HL-60 cells dosed with compound **3a** and viewed by laser scanning confocal microscopy. The red emission produced by excitation of the PS at 458/488 nm was collected through a LP510 filter.

3.4. Dual Type I/II photosensitization

The $^1O_2$ quantum yields (Φ_Δ) for the Ru(II) dyads derived from oligothiophenes increase with increasing n. When $n = 1$, the quantum efficiency of $^1O_2$ generation is approximately 50%, increasing to 75% when $n = 2$, and unity when $n \geq 3$. Given that the PDT effect in experiments with isolated DNA and in cells increases with increasing n, one might be tempted to implicate singlet oxygen as the major contributor to photosensitization by this class of PSs. However, the luminescence quantum yields in the absence of oxygen for dyads with $n \geq 3$ are less than 0.1%, suggesting that an alternate, oxygen-independent nonradiative pathway dominates the excited state dynamics in this class when oxygen tension is low. This notion is supported by gel mobility shift assays (Fig. 9) carried out in the presence of various scavengers widely accepted as mediators of PDT, particularly for clinical agents such as Photofrin®, Visudyne®, Foscan®, Levulan®, and others. Lane 3 represents baseline DNA photodamage by **3a** under the conditions employed, and lanes 4–6, 7, 8–10, and 11 indicate that the PDT effect is not abrogated by scavengers of $^1O_2$, hydrogen peroxide, hydroxyl radical, and superoxide anion, respectively. When n is reduced to 2,

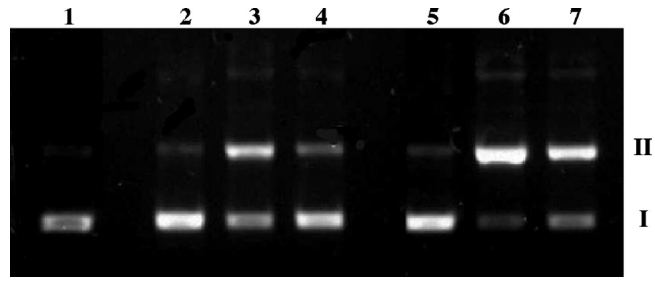

Fig. 10. Gel electrophoretic analysis (1% agarose gel precast with 0.75 μg mL^{-1} ethidium bromide, 1X TAE, 8 V cm^{-1}, 30 min) of PS-mediated pUC19 photocleavage in air-saturated and deoxygenated solution: visible irradiation of pUC19 (20 μM NP in 10 mM Tris·100 mM NaCl, pH 7.4) for 1 h with cool white fluorescent tubes, 21 W·m^2. Lanes 1 (−PS, −hν), 2 (500 μM [Ru(bpy)$_3$]$^{2+}$, −hν), and 5 (2 μM **2a**, −hν) are controls. Lanes 3 (500 μM [Ru(bpy)$_3$]$^{2+}$, +hν) and 6 (2 μM **2a**, +hν) contain samples that were irradiated in air; lanes 4 and 7 are the corresponding samples irradiated in argon.

oxygen-independent, Type I photocleavage persists for **2a** (Fig. 10, Lane 7), but further reduction to $n = 1$ (**1a**) yields a traditional Type II PS with an oxygen dependence comparable to [Ru(bpy)$_3$]$^{2+}$ (Fig. 10, Lane 4).

Compounds **3a** and **3b** act as Type I PSs in the photodynamic inactivation (PDI) of microorganisms such as *S. aureus* and methicillin-resistant *S. aureus* cultured under hypoxic conditions and these Type II effects can also contribute to PDI when oxygen levels are high [17]. Dual Type I/II photosensitization has also been quantified in glioblastoma U87 cells against the clinical agent Levulan® (δ-aminolevulinic acid, or ALA) for this class of PSs with $n \geq 3$ [42], and is responsible for its superior performance over ALA. Retention of a PDT effect, namely, oxygen-independent, Type I activity, in both bacteria and cancer cells represents a significant improvement over the clinical agents mentioned herein, which present an absolute dependence on molecular oxygen for function. The inability of PSs in current clinical use to act as a dual Type I/II agents precludes PDT treatment of hypoxic tissue, which is a salient factor in the limited success of PDT in clinical settings with existing PSs [63]. In fact it has been said that hypoxia might well be the most validated target in cancer therapy [64].

4. Evaluation in cancer cells

4.1. Nuclear localization

Desirable cellular uptake and localization profiles are fundamental to the efficacy of molecular probes and therapeutics [65,66]. Unfortunately, the rational design of molecules with

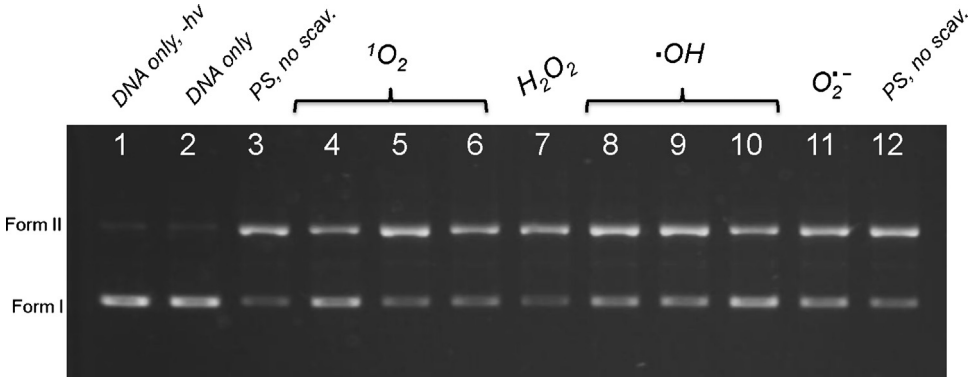

Fig. 9. Effect of different ROS scavengers on the DNA photocleavage of pUC19 (20 μM bases) by compound **3a** (1 μM). Lane 1, DNA only (−hν); lane 2, DNA only (+hν); lane 3, PS (−hν); lane 4, PS, 150 mM DABCO (+hν); lane 5, PS, 150 mM NaN_3 (+hν); lane 6, PS, 150 mM histidine (+hν); lane 7, PS 1000/mL catalase (+hν); lane 8, PS 150 mM mannitol (+hν); lane 9, PS, 150 mM t-butanol (+hν); lane 10, PS, 150 mM DMSO (+hν); lane 11, PS, 1000 U/mL SOD (+hν); lane 12, PS (+hν).

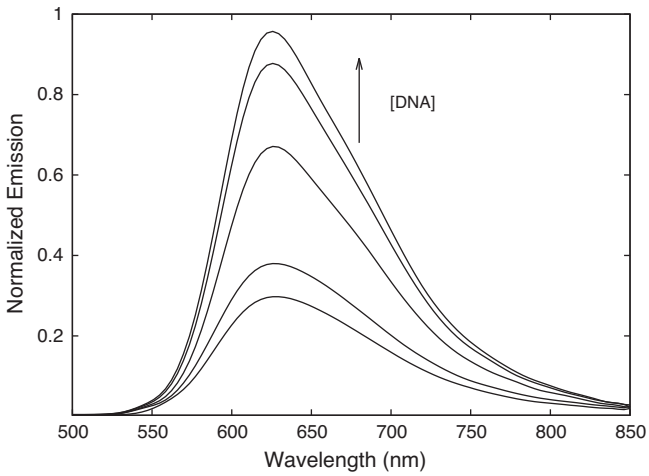

Fig. 11. DNA light-switch effect produced by **3a** (50 μM) binding to CT DNA (2–14 μM bases) in Tris buffer (5 mM Tris·50 mM NaCl) at pH 7.5.

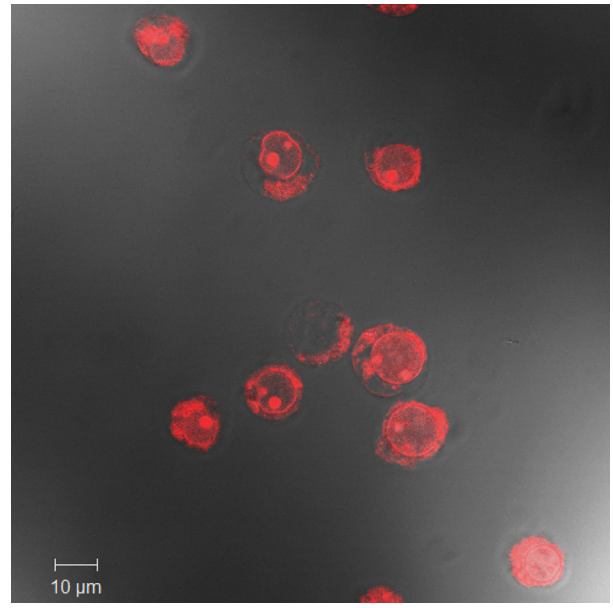

Fig. 12. HL-60 cells dosed with compound **3a** and viewed by laser scanning confocal microscopy. The red emission produced by excitation of the PS at 458/488 nm was collected through a LP510 filter.

the appropriate uptake kinetics and subcellular localization characteristics is not straightforward. In general metal complexes suffer from low cellular uptake and even poorer nuclear penetration [12,67]. Some groups have overcome this problem by shuttling Ru(II) complexes into cells as cargo assisted by targeting moieties such as cell-penetrating peptides (CPPs) [67]. HIV Tat peptide and oligoarginine are examples of CPPs that have been used to facilitate cellular uptake of many cargos, including peptides, proteins, oligonucleotides, plasmids, and peptide nucleic acids [68], as well as potential small-molecule therapeutics such as Ru(II) complexes.

An elegant example of this CPP-assisted delivery was described by Barton et al. [67–69], whereby Ru(II) dipyridophenazine (dppz) complexes were targeted to the nucleus through covalent attachment of D-octaarginine. Without the CPP unit, compounds such as $[Ru(bpy)_2dppz]^{2+}$ accumulate in the cytoplasm. While such strategies have proven effective in producing the desired subcellular localization *in vitro*, it comes as no surprise that appending the basic molecular structure of a potential therapeutic or diagnostic with carrier units and fluorophores, in turn, alters the pharmacokinetic profile of the prodrug. In fact, in many cases the carrier moiety is more spatially demanding than the active cargo itself.

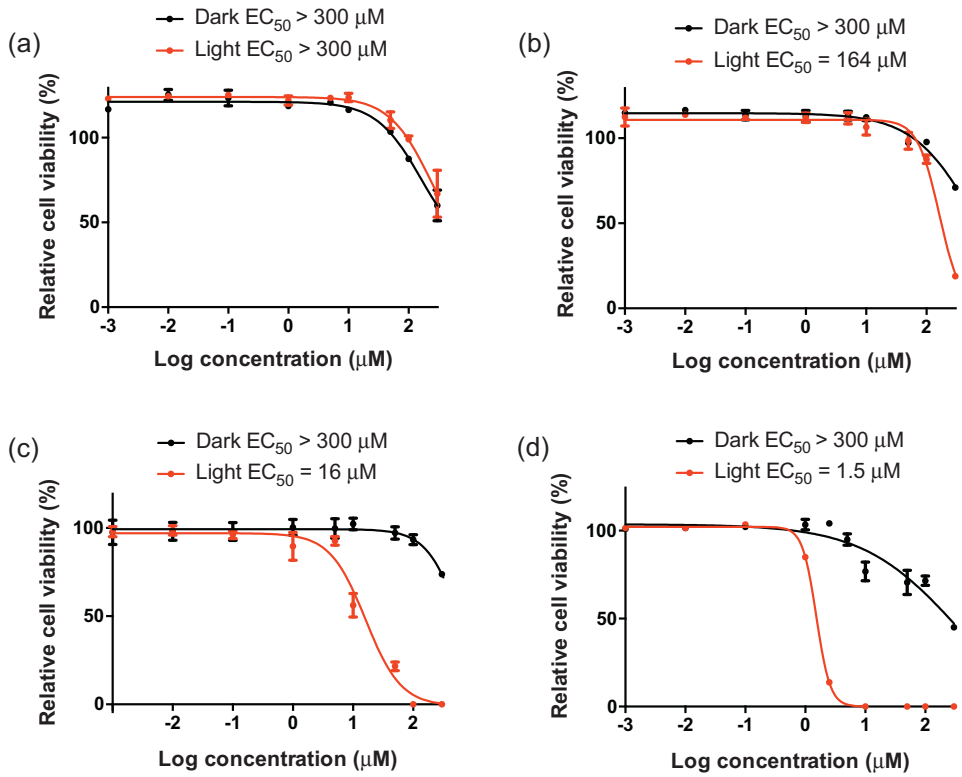

Fig. 13. In vitro PDT dose–response curves for complexes **1b** (a), **2b** (b), **3b** (c) and **4b** (d) in HL-60 cells. Dark (black) and light (red) culture conditions were identical except that the PDT-treated samples were irradiated with 7 J cm^{-2} of visible light with a drug-to-light interval of 1 h.

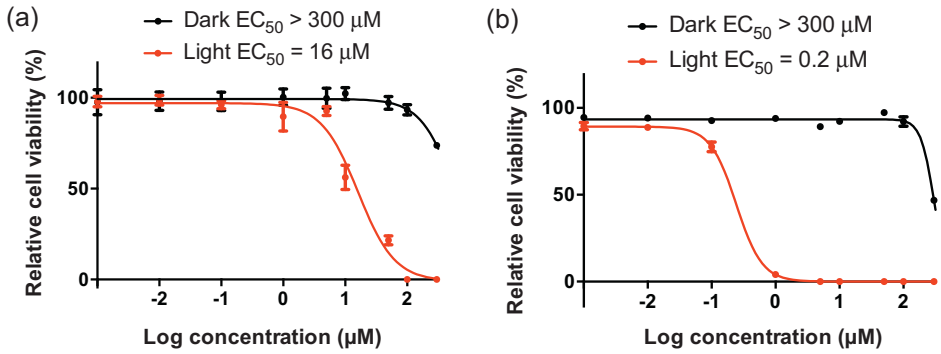

Fig. 14. In vitro PDT dose–response curves for complex **3b** in HL-60 cells. PDT-treated samples were irradiated with (a) 7 J cm^{-2} of visible light with a drug-to-light interval of 1 h or (b) 100 J cm^{-2} of visible light with a drug-to-light interval of 16 h.

Like $[Ru(bpy)_2dppz]^{2+}$, Ru(II) dyads derived from oligothiophene-functionalized ligands exhibit a light switch effect that is triggered by DNA binding. As the conjugation length of the oligothiophene increases so does the emission enhancement upon interaction of the metal complexes with nucleic acids. From $n = 1$ to 3, the corresponding increases in emission are roughly 2, 2.5, and 3.5-fold, respectively (Fig. 11). In live cells, these enhancements are amplified, and confocal microscopy can be used to track the subcellular localization of the dyads without the use of an exogenous fluorophore. Dead and dying cells can be easily distinguished from healthy cells, and the nuclear and nucleoli uptake by viable cells can be tracked with time (Fig. 8). Nuclear penetration is relatively fast, taking place in less than 1 h, and the expanded confocal image (Fig. 12) provides a clearer view of the process. The pronounced nuclear uptake by these PSs and their inducible intracellular luminescence represents a significant improvement in intracellular DNA-targeting without the need for tethered CPPs or fluorescent tags.

Cellular and nuclear uptake increase as light is shone on the cells in the presence of the PSs during the course of a typical microscopy experiment. Some initial photoreactivity at the cell membrane may be responsible for this photosensitization of PS uptake and perhaps the same phenomenon occurs at the nuclear membrane, but any compromise of cell membrane integrity does not lead to cell death during routine imaging times. Facilitation of cellular and nuclear uptake with irradiation presents an orthogonal strategy for minimizing collateral damage to healthy tissue during PDT and is worth further exploration in its own right. Selective uptake and activation of the PS only in the region of irradiation would offer significant improvements over existing clinical PDT agents that are retained in tissues over long periods, resulting in prolonged skin photosensitivity.

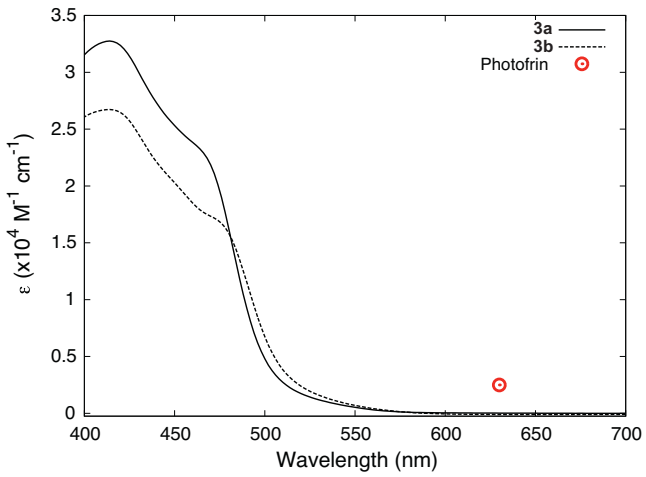

Fig. 15. Electronic absorption comparison of complexes **3a** and **3b** ([PS] = 20 μM) in aqueous buffer (5 mM Tris·50 mM NaCl, pH 7.4). The molar extinction coefficient (630 nm) for Photofrin is marked for comparison.

4.2. In vitro PDT

A human leukemia cancer cell line (HL-60) and the Alamar Blue (AB) cell viability test were used to quantify the *in vitro* PDT effect for these Ru(II) dyads of varying *n*. The HL-60 cell line is a standard model used [28,13,9] to assess photodynamic activity by PSs in live cells. In our conditions, HL-60 cells are dosed with PS concentrations of 1 nM to 300 μM (the upper limit due to solubility constraints). The effective concentration to reduce cell viability by 50% (EC_{50}) is then assessed with no light treatment and following

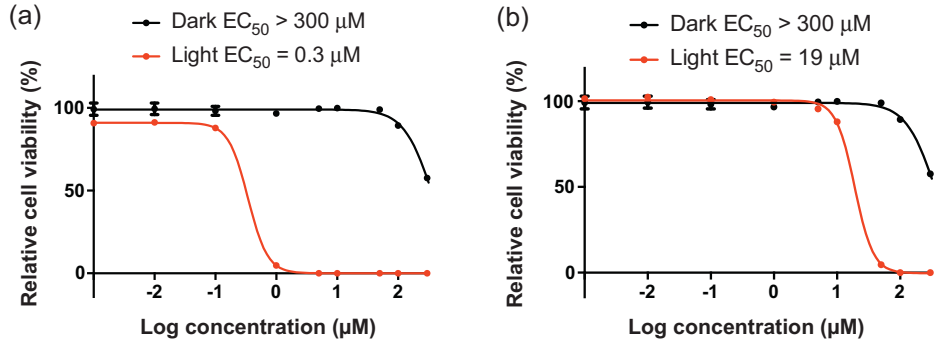

Fig. 16. In vitro PDT dose–response curves for complex **3b** in HL-60 cells. PDT-treated samples were irradiated with 100 J cm^{-2} of (a) visible light or (b) red light with drug-to-light intervals of 16 h.

various drug-to-light intervals ($t_{h\nu}$). From the dark and light cytotoxicity profiles, a phototherapeutic index (PI) can be calculated as the ratio of the dark EC_{50} to the light EC_{50}, and it represents the effective therapeutic range of the PS where dark toxicity is minimal.

The dark cytotoxicity of this family is very low (Fig. 13). Others have cited EC_{50} values greater than 300 μM as virtually nontoxic [9], and all of the Ru(II) dyads discussed herein (Figs. 2 and 3) have dark EC_{50} values that exceed 300 μM. In the case of **1b** where $n = 1$, there is no PDT effect in cells with a notably short drug-to-light interval ($t_{h\nu} = 1$ h). Under identical conditions, $n = 2$ gives a light toxicity of 164 μM (PI>1.8). On going from **2b** to **3b**, increasing n from 2 to 3, the light toxicity increases ten-fold as does the PI. For **4b** ($n = 4$), the light EC_{50} value is as low as 1.5 μM (PI>200). When $n \geq 4$, decreased solubility in aqueous media precludes accurate assessment of cytotoxicity parameters so $n = 5$ and larger is not discussed herein. However, a 200-fold increase in light cytotoxicity with no corresponding effect on the dark toxicity is a remarkable improvement on going from $n = 1$ to 4 in this family of dyads, and the trend is analogous for **1a**–**4a**. The desire to focus on the dmb coligand stems from a slight improvement in water solubility over their bpy counterparts.

The comparison among **1b**–**4b** (Fig. 13) was carried out with a notably short pre-PDT incubation period of only 1 h to illustrate the effectiveness of **3b** and **4b**. PSs employed for *in vitro* PDT typically require much longer drug-to-light intervals (16–24 h) due to slow cellular uptake, whereby light presumably does not act to facilitate subcellular localization as is observed in this series. When the PDT treatment is optimized by increasing the light dose from 7 J cm^{-2} to 100 J cm^{-2} and the drug-to-light interval to 16 h (Fig. 14b), the light EC_{50} value for **3b** is 200 nM, and the PI is greater than 1500. These unusually large therapeutic indices and extremely potent light cytotoxicities appear to be a general feature of Ru(II) dyads characterized by lowest-lying ^{3}IL excited states [28], which are highly sensitive to trace amounts of oxygen and also exhibit dual Type I/II switching behavior [13]. Another phenomenon that we have recently documented for Ru(II) dyads possessing low-lying ^{3}IL states is their capacity for multiwavelength PDT, particularly with wavelengths for which their molar extinction coefficients are very low [70]. The absorption spectra for **3a** and **3b** (Fig. 15) show very little absorption in the phototherapeutic window (600–850 nm) where tissue is most transparent. Molar extinction coefficients for these complexes are on the order of 10 $M^{-1}cm^{-1}$ at 630 nm, where Photofrin® has an absorption cross-section of 2250 $M^{-1}cm^{-1}$ [71]. Nevertheless, it is possible to generate PDT with red light (625 nm), and the effect is respectable with a light EC_{50} of 19 μM and a PI exceeding 15 (Fig. 16). In the glioblastoma U87 cell line, the potency is even better, with light EC_{50} values as low as 1 μM and PIs that exceed that of Photofrin®.

While the precise mechanism for cell death remains to be elucidated, the nuclear localization confirmed by microscopy combined with a size distribution analysis on the PDT-treated cells point toward apoptosis (Fig. 17). Typically cells undergoing necrosis swell while cells responding to apoptotic signaling pathways shrink. Healthy HL-60 cells have mean cell diameters centered around 11 μm, and the PDT-treated cells using PSs **3a** or **3b** shrink to 4.6 μm before being lost on the image to phagocytosis or as cellular debris.

5. Evaluation in animals: *in vivo* PDT

The ability of a PS to act effectively and impressively in isolated cells does not *a priori* translate to a good *in vivo* PDT agent. Obviously, absorption, distribution, metabolism, and excretion (ADME) are crucial factors that govern whether a PS will be systemically toxic to its host. In the case of the Ru(II) dyads derived from oligothiophenes, however, good *in vitro* activity does translate to

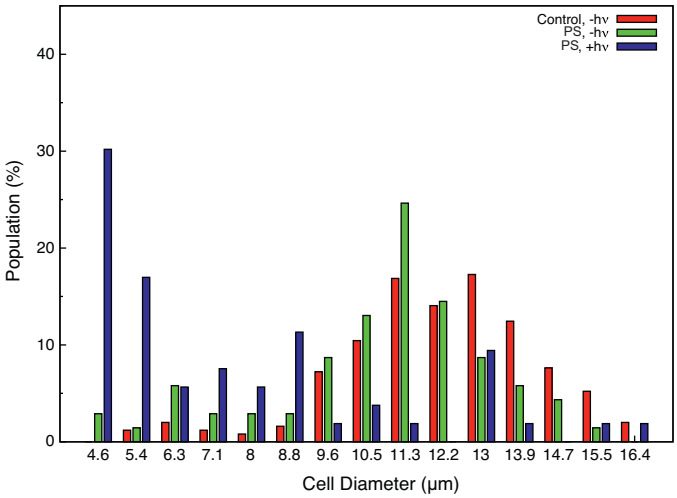

Fig. 17. Size distribution of PS-dosed HL-60 cells at 40 h post PDT treatment.

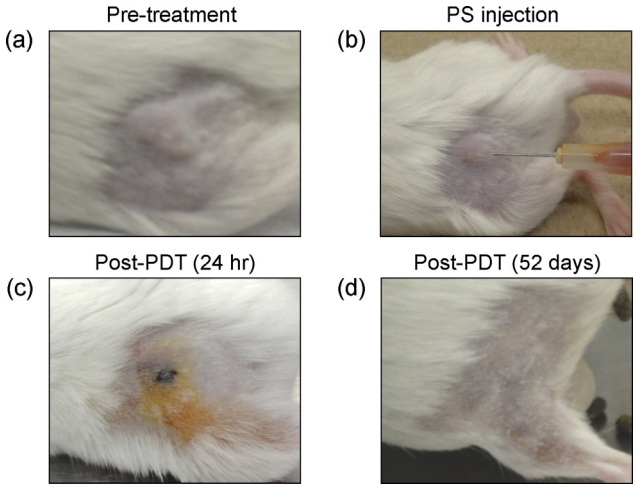

Fig. 18. No signs of tumor at 52 days post PDT treatment with **3b** (53 mg kg^{-1}) and 525-nm continuous wave light (192 J cm^{-2}).

excellent *in vivo* PDT in a rodent model. *In vivo* MTD_{50} values were determined for **3a** and **3b** using a standard dose escalation scheme in order to ascertain dark toxicity toward the animals. MTD_{50} values represent the maximum tolerated dose, where 50% of the animals survive the dose. The MTD_{50} values for **3a** and **3b** are 36 mg kg^{-1} and 103 mg kg^{-1}, respectively. For comparison, the administered dose for commonly employed PSs such as Photofrin® in rats is 12.5 mg kg^{-1} [72], and the toxicity in humans is close to 2 mg kg^{-1} [73].

The relatively low dark toxicity of **3b** in particular combined with its increased water solubility relative to **3a** is an attractive starting point for further development of a viable PDT agent for human use. When mice are inoculated with colon carcinoma cells (CT26.WT), subcutaneous tumors form readily. When the subcutaneous colon tumors reached 5.0 ± 0.5 mm in long-axis diameter, 53 mg kg^{-1} of PS **3b** was intratumorally injected (Fig. 18). Subsequent PDT treatment with 525-nm continuous wave (CW) light (192 J cm^{-2}) resulted in complete tumor destruction with no evidence of tumors even at 52 days post treatment. The corresponding Kaplan–Meier curves describing animal survival with PDT treatment using dyads **3a** and **3b** (Fig. 19) demonstrate that *in vivo* PDT with these PSs yields significant improvement in animal survival over control animals with as little as 2 mg kg^{-1} and 5 mg kg^{-1} PS, respectively. These doses are 2–6 times lower than the doses at

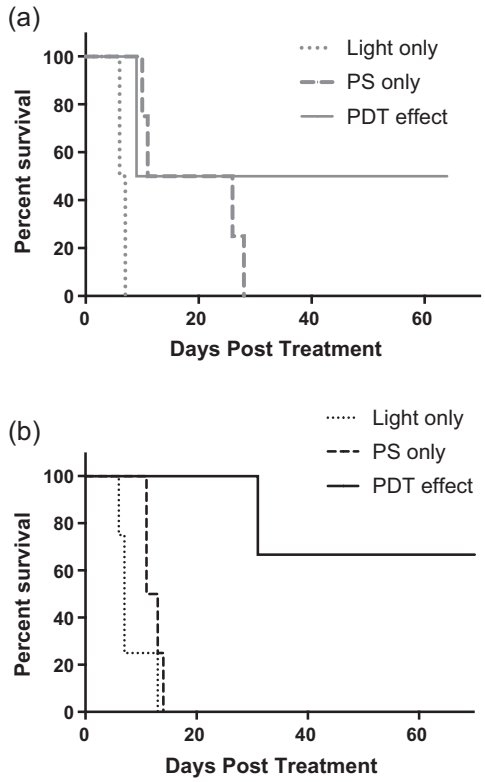

Fig. 19. Kaplan-Meier survival curves for mice bearing tumors post PDT treatment with **3a** (a) or **3b** (b) and 525 nm light.

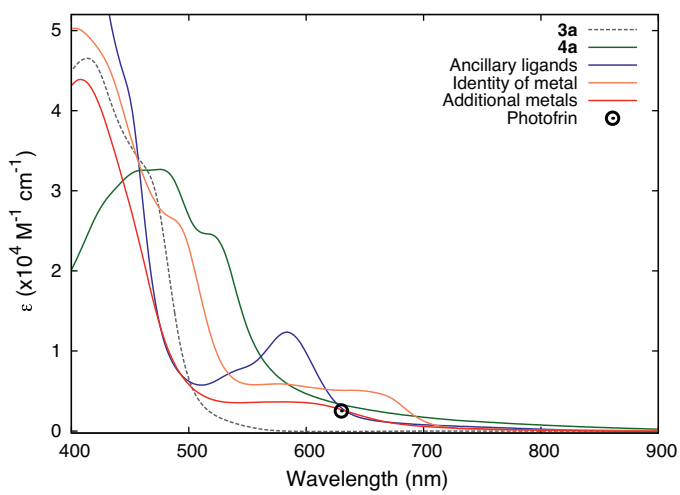

Fig. 20. Electronic absorption spectra of **3a** and several of its structural derivatives at 20 μM in acetonitrile. The molar extinction coefficient (630 nm) for Photofrin is marked for comparison.

which Photofrin® are administered in similar pre-clinical models, and 40–100 times lower than those for Levulan®.

The PDT parameters can be optimized further for treatment in the PDT window given that these dyads with $n \geq 3$ generate red PDT despite the fact that they do no absorb red light substantially. We have achieved this red PDT effect in animals as well. Given that the Ru(II) framework is modular in design, the dyads are easily modified to alter absorption of light as well as photobiological properties and ADME profiles. Increasing the number of thiophenes from $n = 3$ as in **3a** or **3b** to $n = 4$ (**4a** or **4b**) increases the molar extinction coefficients of the dyads at 630 nm to be on par with that of Photofrin® (Fig. 20). Similar improvements can be invoked by altering the ancillary ligands (blue curve), changing the identity of the central metal ion (orange curve), and adding additional metals to yield mixed metal complexes (red curve) [74,42]. However, very subtle, and certainly gross, structural changes can have profound effects on the photobiological activities of the PSs, and one cannot easily extrapolate the *in vivo* PDT efficacy from the simpler *in vitro* PDT experiments, even 3D tumor spheroid models. Therefore, we use *in vitro* PDT to narrow our libraries to acceptable numbers for animal experiments, but *in vivo* investigation is crucial for ascertaining the true potential of a PS for clinical PDT. Moreover, the *in vivo* dosimetry and the light component of PDT are just as important as the PS—perhaps, arguably, more important. The PS may set a maximum threshold of PDT that can be obtained, but its *in vitro* potency is rarely achieved in live animal models owing to problems inherent to *in vivo* dosimetry. Furthermore, the ideal PS, light treatment, and protocol will be different for different cancers and even different among phenotypes of the same cancer. Consequently, identification of promising PSs for PDT necessarily requires a multidisciplinary approach for further development, and medical biophysicists and cancer specialists are critical in moving forward.

6. Summary and outlook

Metal-based PSs offer a versatility that is far beyond what can be achieved with traditional organic systems that are in clinical use for PDT. Their modular architecture can yield a breadth of photoreactivity with only minor structural modification. The addition of a few methyl groups, for example, can turn a $^1O_2$ generator into a metal complex that covalently modifies DNA through the formation of photoadducts. More recently, systems have been documented that are capable of partitioning their excited state reactivity between oxygen-dependent and oxygen-independent mechanisms depending on local oxygen tension and environment, overcoming a significant drawback associated with organic PSs. While significant effort has been directed toward moving the absorption of these metal-based PSs into the PDT window, Ru(II) dyads derived from a variety of π-expansive ligands are surprisingly effective with red light activation despite minimal absorption in this wavelength region. The striking potency responsible for this phenomenon has eliminated the one advantage the porphyrin-based PSs held, namely, activation in the PDT window. The Ru(II) dyads described in this review demonstrate these points and also show that nuclear targeting is possible without elaborate carrier systems. Moreover, the *in vitro* activity of these metal complexes translates to *in vivo* rodent models, with MTD_{50} values that are superior to Photofrin®. These dyads are currently undergoing the final stages of pre-clinical optimization for human Phase 1 studies this year and will pave the way for a new class of PSs that may position PDT as a mainstream cancer treatment.

Acknowledgments

S.A.M., G.S., S.M., R.H., J.C., H.Y., R.D., C.S., and L.C. thank the Canadian Institutes of Health Research, the Natural Sciences and Engineering Research Council of Canada, the Canadian Foundation for Innovation, the Nova Scotia Research and Innovation Trust, and the Beatrice Hunter Cancer Research Institute for financial support and Prof. Todd Smith for use of his cell and tissue culture facility. We also thank Profs. Edith Glazer (Univ. of Kentucky) and Douglas Magde (Univ. of California San Diego) for insightful discussions.

References

[1] R. Bonnett, Chemical Aspects of Photodynamic Therapy, Gordon and Breach Science Publishers, Amsterdam, 2000.
[2] M.H. Hanigan, P. Devarajan, Cancer Ther. 1 (2003) 47–61.

[3] R.Y. Tsang, T. Al-Fayea, H.-J. Au, Drug Saf. 32 (2009) 1109–1122.
[4] S.R. McWhinney, R.M. Goldberg, H.L. McLeod, Mol. Cancer Ther. 8 (2009) 10–16.
[5] M. Ethirajan, Y. Chen, P. Joshi, R.K. Pandey, Chem. Soc. Rev. 40 (2011) 340–362.
[6] Y. Sun, L.E. Joyce, N.M. Dickson, C. Turro, Chem. Commun. 46 (2010) 2426–2428.
[7] Y. Sun, L.E. Joyce, N.M. Dickson, C. Turro, Chem. Commun. 46 (2010) 6759–6761.
[8] A.A. Holder, S. Swavey, K.J. Brewer, Inorg. Chem. 43 (2004) 303–308.
[9] B.S. Howerton, D.K. Heidary, E.C. Glazer, J. Am. Chem. Soc. 134 (2012) 8324–8327.
[10] E. Wachter, D.K. Heidary, B.S. Howerton, S. Parkin, E.C. Glazer, Chem. Commun. 48 (2012) 9649–9651.
[11] E. Wachter, B.S. Howerton, E.C. Hall, S. Parkin, E.C. Glazer, Chem. Commun. 50 (2014) 311–313.
[12] E.C. Glazer, Israel J. Chem. 53 (2013) 391–400.
[13] S. Monro, J. Scott, A. Chouai, R. Lincoln, R. Zong, R.P. Thummel, S.A. McFarland, Inorg. Chem. 49 (2010) 2889–2900.
[14] K. Plaetzer, B. Krammer, J. Berlanda, F. Berr, T. Kiesslich, Lasers Med. Sci. 24 (2009) 259–268.
[15] D.S. Wishart, Drugs Res. Dev. 8 (2007) 349–362.
[16] Y. Liu, R. Hammitt, D.A. Lutterman, L.E. Joyce, R.P. Thummel, C. Turro, Inorg. Chem. 48 (2009) 375–385.
[17] Y. Arenas, S. Monro, G. Shi, A. Mandel, S. McFarland, L. Lilge, Photodiag. Photodyn. Ther. 10 (2013) 615–625.
[18] J. Nguyen, Y. Ma, T. Luo, R.G. Bristow, D.A. Jaffray, Q.-B. Lu, Proc. Natl. Acad. Sci. U. S. A. 108 (2011) 11778–11783.
[19] W. Lu, D.A. Vicic, J.K. Barton, Inorg. Chem. 44 (2005) 7970–7980.
[20] M.S. Wrighton, D.L. Morse, L. Pdungsap, J. Am. Chem. Soc. 97 (1975) 2073–2079.
[21] P.J. Giordano, S.M. Fredericks, M.S. Wrighton, D.L. Morse, J. Am. Chem. Soc. 100 (1978) 2257–2259.
[22] S.M. Fredericks, J.C. Luong, M.S. Wrighton, J. Am. Chem. Soc. 101 (1979) 7415–7417.
[23] L. Pdungsap, M.S. Wrighton, J. Organomet. Chem. 127 (1977) 337–347.
[24] W.E. Ford, M.A.J. Rodgers, J. Phys. Chem. 96 (1992) 2917–2920.
[25] N.D. McClenaghan, Y. Leydet, B. Maubert, M.T. Indelli, S. Campagna, Coord. Chem. Rev. 249 (2005) 1336–1350.
[26] D.V. Kozlov, D.S. Tyson, C. Goze, R. Ziessel, F.N. Castellano, Inorg. Chem. 43 (2004) 6083–6092.
[27] C. Goze, D.V. Kozlov, D.S. Tyson, R. Ziessel, F.N. Castellano, New J. Chem. 27 (2003) 1679–1683.
[28] R. Lincoln, L. Kohler, S. Monro, H. Yin, M. Stephenson, R. Zong, A. Chouai, C. Dorsey, R. Hennigar, R.P. Thummel, S.A. McFarland, J. Am. Chem. Soc. 135 (2013) 17161–17175.
[29] D.S. McClure, J. Chem. Phys. 17 (1949) 665–666.
[30] J. Pérez-Prieto, L.P. Pérez, M. González-Béjar, M.A. Miranda, S.-E. Stiriba, Chem. Commun. (2005) 5569–5571.
[31] R.S. Becker, J. Seixas de Melo, A.L. Maanita, F. Elisei, J. Phys. Chem. 100 (1996) 18683–18695.
[32] R.A.J. Janssen, D. Moses, N.S. Sariciftci, J. Chem. Phys. 101 (1994) 9519–9527.
[33] M.B. Majewski, N.R. de Tacconi, F.M. MacDonnell, M.O. Wolf, Inorg. Chem. 50 (2011) 9939–9941.
[34] M.B. Majewski, N.R. de Tacconi, F.M. MacDonnell, M.O. Wolf, Chem. Eur. J. 19 (2013) 8331–8341.
[35] C. Moorlag, B. Sarkar, C.N. Sanrame, P. Bäuerle, W. Kaim, M.O. Wolf, Inorg. Chem. 45 (2006) 7044–7046.
[36] J.C. Scaiano, R.W. Redmond, B. Mehta, J.T. Arnason, Photochem. Photobiol. 52 (1990) 655–659.
[37] J.C. Scaiano, A. MacEachern, J.T. Arnason, P. Morand, D. Weir, Photochem. Photobiol. 46 (1987) 193–199.
[38] J.P. Reyftmann, J. Kagan, R. Santus, P. Morliere, Photochem. Photobiol. 41 (1985) 1–7.
[39] M. Ciofalo, S. Petruso, D. Schillaci, Planta Med. 62 (1996) 374–375.
[40] T.K. Saito, M. Takahashi, H. Muguruma, E. Niki, K. Mabuchi, J. Photochem. Photobiol. B, Biol. 61 (2001) 114–121.
[41] N.R. Krishnaswamy, C.S.S.R. Kumar, Ind. J. Chem. 32B (1993) 766–771.
[42] S.A. McFarland, Metal-based Thiophene Photodynamic Compounds and Their Use. US provisional patent #61624391 filed April 15, 2012, PCT/US13/36595 filed April 15, 2013.
[43] J.C. Wang, Nat. Rev. Mol. Cell Biol. 3 (2002) 430–440.
[44] R. Palchaudhuri, P.J. Hergenrother, Curr. Opin. Biotechnol. 18 (2007) 497–503.
[45] M.A. Fuertes, J. Castilla, C. Alonso, J.M. Prez, Curr. Med. Chem. 10 (2003) 257–266.
[46] A. Binter, J. Goodisman, J.C. Dabrowiak, J. Inorg. Biochem. 100 (2006) 1219–1224.
[47] M.V. Keck, S.J. Lippard, J. Am. Chem. Soc. 114 (1992) 3386–3390.
[48] O. Vrana, V. Boudny, V. Brabec, Nucl. Acids Res. 24 (1996) 3918–3925.
[49] Y. Pommier, Nat. Rev. Cancer 6 (2006) 789–802.
[50] B.K. Sinha, Drugs 49 (1995) 11–19.
[51] Y. Pommier, ACS Chem. Biol. 8 (2013) 82–95.
[52] S. Lheureux, B. Clarisse, V. Launay-Vacher, K. Gunzer, C. Delcambre-Lair, K. Bouhier-Leporrier, L. Kaluzinski, D. Maron, M.-D. Ngo, S. Grossi, B. Dubois, G. Zalcman, F. Joly, Anticancer Drugs 22 (2011) 919–925.
[53] H.-P. Lipp, Anticancer Drug Toxicity: Prevention, Management, and Clinical Pharmacokinetics, Taylor & Francis, 1999.
[54] M. Vanneman, G. Dranoff, Nat. Rev. Cancer 12 (2012) 237–251.
[55] K. Malinowsky, J. Cancer (2011) 26.
[56] W.H. Ang, P.J. Dyson, Eur. J. Inorg. Chem. 2006 (2006) 3993.
[57] R.J. Gillies, D. Verduzco, R.A. Gatenby, Nat. Rev. Cancer 12 (2012) 487–493.
[58] M. Das Thakur, F. Salangsang, A.S. Landman, W.R. Sellers, N.K. Pryer, M.P. Levesque, R. Dummer, M. McMahon, D.D. Stuart, Nature 494 (2013) 251–255.
[59] G. Hintermann, H.M. Fischer, R. Crameri, R. Htter, Plasmid 5 (1981) 371–373.
[60] T. Schmidt, K. Friehs, M. Schleef, C. Voss, E. Flaschel, Anal. Biochem. 274 (1999) 235–240.
[61] V. Cepeda, M.A. Fuertas, J. Castilla, C. Alonso, C. Quevedo, J.M. Perez, Anticancer Agents Med. Chem. 7 (2007) 3–18.
[62] K.E. Wright, A.J. MacRobert, J.B. Phillips, Photochem. Photobiol. 88 (2012) 1539–1545.
[63] P. Vaupel, A. Mayer, Cancer Metastasis Rev. 26 (2007) 225–239.
[64] W.R. Wilson, M.P. Hay, Nat. Rev. Cancer 11 (2011) 393–410.
[65] N.S. Bryce, J.Z. Zhang, R.M. Whan, N. Yamamoto, T.W. Hambley, Chem. Commun. (2009) 2673–2675.
[66] F. Madani, S. Lindberg, Ü. Langel, S. Futaki, A. Gräslund, J. Biophys. 2011 (2011) 1–10.
[67] C.A. Puckett, J.K. Barton, Bioorg. Med. Chem. 18 (2010) 3564–3569.
[68] C.A. Puckett, J.K. Barton, J. Am. Chem. Soc. 131 (2009) 8738–8739.
[69] J. Brunner, J.K. Barton, Biochemistry 45 (2006) 12295–12302.
[70] H. Yin, M. Stephenson, J. Gibson, E. Sampson, G. Shi, T. Sainuddin, S. Monro, S.A. McFarland, Inorg. Chem. (2014), http://dx.doi.org/10.1021/ic5002368, in press.
[71] M. Matsuoka, Infrared Absorbing Dyes, Springer, New York, 1990.
[72] M.O. Dereski, M. Chopp, Q. Chen, F.W. Hetzel, Photochem. Photobiol. 50 (1989) 653–657.
[73] M.H. Schmidt, G.A. Meyer, K.W. Reichert, J. Cheng, H.G. Krouwer, K. Ozker, H.T. Whelan, J. Neurooncol. 67 (2004) 201–207.
[74] S.A. McFarland, Metal-based Coordination Complexes as Photodynamic Compounds and Their Use, US provisional patent #61801674 filed March 15, 2013, PCT/US14/30194 filed March 17, 2014.